Cell. Mol. Biol. (ISSN: 1165-158X)

Journal Homepage: www.cellmolbiol.org

Cellular and Molecular Biology

Original Article

Analysis of the heterologous expression, localization, and cellular response to the Zika virus E protein in vitro

David Hernán Martínez-Puente[1], Manuel Lara-Lozano[1], Nicolás Aguirre-Pineda[1], María de Jesús Loera-Arias[2], Juan E. Ludert[3], José Segovia[1*]

[1] Departamento de Fisiología, Biofísica y Neurociencias, Centro de Investigación y de Estudios Avanzados del IPN, CDMX 07360, México
[2] Departamento de Histología, Facultad de Medicina, Universidad Autónoma de Nuevo León, Monterrey 64460, México
[3] Departamento de Infectómica y Patogénesis Molecular, Centro de Investigación y de Estudios Avanzados del IPN, CDMS 07360, México

Article Info

Article history:

Received: February 08, 2024
Accepted: May 23, 2024
Published: October 31, 2024

Use your device to scan and read the article online

Abstract

Zika virus (ZIKV) infection has been associated with damage to neural stem cells in microcephaly in newborns. The virus possesses specific tropism for glioma stem cells mediated by the ZIKV E protein. This infection causes endoplasmic reticulum stress and activation of the unfolded protein response (UPR). However, the cellular response to the expression of the ZIKV E protein alone is unknown. Therefore, in this study, we determined the effect of the expression of the ZIKV E protein on cellular responses and its subcellular localization in HEK-293T cells, due to their use as a biotechnological tool for cellular and lentiviral therapy. We observed that the ZIKV E protein is synthesized in the cytoplasm and inserted into the endoplasmic reticulum (ER), without causing activation of the UPR or cell death, and it is finally transported and located in the cell membrane. Moreover, the expression of the ZIKV E protein does not induce UPR or apoptosis in glioma cells. These results help us to better understand the characteristics of this protein and its possible use as a biotechnological tool for the creation of different gene therapy strategies, vaccines, and synthetic vectors with tropism for neural and glioma stem cells.

Keywords: UPR, Zika, ZIKV E protein, ER stress, cell death.

1. Introduction

The ZIKV was first isolated in 1947 from a sentinel monkey in the Zika forest of Uganda [1], and the first human epidemic outbreak was reported in 2007 in the Yap islands. However, a few years ago ZIKV was introduced in the Americas causing an alarming number of cases of microcephaly in newborns from mothers infected with the virus [2]. The ZIKV is responsible for microcephaly in animal models by eliminating neural progenitor cells [3, 4]. This phenomenon is directly related to chronic stress in the endoplasmic reticulum (ER) owing to the overburden of protein production during virus infection [5, 6]. ZIKV not only has a tropism for neural stem cells but also a tropism for glioma stem cells has been observed, which is why it is capable of preventing the appearance of secondary tumors derived from post-surviving glioblastoma stem cells [7]. The ZIKV E protein has been identified as responsible for these tropisms [8, 9]; therefore, it is of great importance to better understand its biological characteristics and cellular effects.

The ZIKV belongs to the *Flaviviridae* family, genus *Flavivirus*, which consists of enveloped icosahedral viruses, with a diameter of approximately 50 nm, that contain a single positive 9- to 12-kb RNA strand genome [10]. The ZIKV is mainly transmitted to humans through the bite of infected *Aedes aegypti* mosquitoes [11]. However, other mosquito species within the *Aedes* genus (*A. africanus*, *A. luteocephalus*, *A. furcifer*, *A. taylori*, and *A. albopictus*) also have a high potential to spread the virus [12]. The viral infection in adults and children usually results in a mild, self-limited febrile illness [13].

In some cases, in addition to mosquito bites, women have been also infected with ZIKV through sexual contact with people affected with the disease, and infection during the first pregnancy trimester, has been associated with an increase in newborns with microcephaly [14, 15]. Microcephaly is a neurological developmental disorder, with an evident reduction in the size of brain mass and intellectual disability caused by little cell proliferation, induced by the death of progenitor cells and their neuronal progeny

* Corresponding author.
E-mail address: jsegovia@fisio.cinvestav.mx (J. Segovia).
Doi: http://dx.doi.org/10.14715/cmb/2024.70.10.11

[16]. Prenatal analyses of placenta and amniotic fluid from ZIKV-infected women and blood samples from their newborns with microcephaly were positive for ZIKV RNA. In addition to these data in humans, several of these characteristics have also been replicated in animal models, indicating transplacental transmission of ZIKV [17–19].

The ZIKV genome is translated into a single polyprotein of 3,423 amino acids, that after proteolytic processing by viral and host proteases, generates three structural proteins: capsid (C), membrane precursor (prM), and the envelope protein (E); and seven non-structural proteins named NS1, NS2A, NS2B, NS3, NS4A, NS4B, and NS5 [20]. Structural proteins make up the virion, while non-structural proteins participate in genome replication, packaging, and modulation of cell innate immunity [21, 22].

The ZIKV E is a glycoprotein of approximately 54 kDa, it is formed by three domains: the EDI domain which is β-barrel shaped, located centrally in the protein monomer, and acts in conformational processes during infection [23], the EDII domain which is finger-shaped, and causes the stability of dimers and participates in membrane fusion and endocytosis during infection through the fusion peptide, in addition to being the prM chaperone-binding domain [21, 24], and the EDIII domain, which has a form similar to that of an immunoglobulin, participates in the first contact between the virus and host cells [25, 26].

The ZIKV E protein is the virion cell-binding protein [24, 27], as it interacts with the αvβ5 integrin receptor on glioblastoma stem cells [28, 29]; however, it has been reported that the AXL receptor also participates in ZIKV early events during infection [30–32]. Therefore, directing therapeutic vectors that use ZIKV E protein as a specific ligand can provide a specific and efficient strategy to battle aggressive human tumors of the central nervous system [33]. This strategy has been used previously, adding different, other than the ZIKV E, viral envelope glycoproteins in a vector to provide a tropism for a specific cell or tissue [34–36].

ZIKV replication takes place in close association with the ER [37], and after processing, several viral proteins, including E, remain in the ER lumen. Activation of the UPR in ZIKV and other flavivirus-infected cells has been reported, inhibiting the formation of stress granules [38, 39]. In vertebrates, the presence of high levels of UPR, in apical progenitor cells produces the first neurons, known as direct neurogenesis. In later stages, mammals show a decrease in the UPR, allowing the formation of basal progenitor cells that give rise to new neurons; this phenomenon is referred to as indirect neurogenesis. The replication of the ZIKV maintains the UPR elevated by indirectly inhibiting the formation of neurons. This mechanism has been related to the death of neural stem cells in microcephaly [40].

The UPR is the ER stress response, which is characterized as a mechanism for restoring homeostasis caused by an imbalance in cellular proteostasis (homeostasis of protein synthesis, structuring, transport, and degradation) [41]. This process is induced by factors, such as viral infections [42], sudden temperature changes, and oxidizing environments [43]. The UPR has three functions: shutdown protein synthesis induced by the activation of PERK [44, 45], the over-expression of chaperones such as GRP78 for correct protein folding [46, 47], and membrane protein synthesis via the activation of IRE1α and ATF6 to increase the size of the ER. If this is not sufficient to restore homeostasis, the degradation of misfolded proteins is carried out through endoplasmic reticulum-associated degradation (ERAD), or, finally, cell death occurs by apoptosis [48–50]. During ZIKV infections, the ZIKV E protein has been observed to interact with the chaperone GRP78, which plays a mediating role in the internalization of the virus and participates in viral replication [51, 52]. However, there is no evidence that the expression of the ZIKV E protein *per se* leads to the overexpression of this chaperone or UPR activation. Therefore, it is important to elucidate the role of the cellular pathways involved in ZIKV E protein synthesis and processing, to assess cellular homeostasis and to identify appropriate vectors to carry out these therapies.

Due to the great interest in the use of ZIKV E protein to direct different therapies to target cells such as those derived from glioblastoma, we sought to characterize the cellular response in terms of stress or death, to the expression of this protein in HEK-293T cells; a line which is used in most therapeutic strategies and the production of recombinant proteins [53]. In addition, we also examined the UPR and apoptosis responses in human glioma cells expressing ZIKV E.

2. Materials and methods

2.1. Cell lines

The HEK293T cell line, derived from human embryonic kidney (ATCC, cat# CRL-3216), and the U-87 MG, a human glioma cell line (ATCC, cat# HTB-14) were maintained in Dulbecco's Modified Eagle's Medium (DMEM, high glucose) (GIBCO, cat# 12800-017) supplemented with 10% fetal bovine serum (FBS) (Gibco, cat# 16000-044), 1 mM L-glutamine (Sigma-Aldrich, cat# 35050061), and 100 U/mL penicillin/100µg streptomycin (Gibco, cat# 15140-122). Mosquito *Aedes albopictus* C6/36 cells (ATCC, cat# CRL-1660) were grown in Eagle's minimum essential medium (EMEM), supplemented with 10% FBS and 100 U/mL penicillin-streptomycin. Mammalian and mosquito cell cultures were maintained at 37 °C, and 28 °C respectively, in a 5% CO_2 atmosphere.

2.2. Expression vector

The ZIKV (ZIKV/Homosapiens/MEX/2016/mex24) was propagated in C6/36 cells. Genomic viral RNA was purified from infected C6/36 cell supernatants using the QIAamp Viral RNA kit (QIAGEN, cat# 52906), following the supplier's protocol, in a Type II biosafety hood. The purified genome was then treated with DNase I (Invitrogen, cat# 18068015), viral cDNA was synthesized using random primers (50 µM) and Superscript III reverse transcriptase (Invitrogen, cat# 10777019) as previously described [54].

The gene encoding the ZIKV E protein was amplified using endpoint PCR. A Kozak sequence with the methionine codon was introduced at the 5' region with the forward primer: 5'-TACCACCATGATCAGGTGCATAGGAGTCAGC-3'. A stop codon and the *XhoI* recognition sequence were incorporated at the 3' region using the reverse primer: 5'-ACTCGAGCTAAGCAGAGACGGCTGTGGAT-3'. Briefly, for the PCR reaction, 0.6 µL of AccuPrime Pfx polymerase (Invitrogen, cat# 12344024), 5 µL of the 10x Buffer, 5 µL of DMSO, 0.8 µL of each primer (10 µM), 2 µL of viral cDNA, and molecular biolo-

gy-grade water to reach a total volume of 50 µL were used. The thermal cycler conditions consisted of an initial step at 94° C for 5 min, followed by 40 cycles of three steps at 94° C for 30 s, 58°C for 30 s, and 68° C for 60 s, with a final step at 68° C for 5 min.

The resulting 1,531 bp amplicon was cloned into the pCR4 vector using TOPO-Blunt technology (Invitrogen, cat# 450031) following the supplier's instructions. Subsequently, the E-Protein (E-ZIKA) transgene was subcloned into the pcDNA 3.0 plasmid through restriction with *EcoRI* (NEB, cat# R0101S) and *XhoI* (NEB, cat# R0146S), followed by ligation with T4 ligase (ThermoFisher, cat# 15224017). The final product was sequenced using the Sanger method, and the resulting sequence confirmed 100% identity to the ZIKV E gene of the ZIKV isolate ZIKV/Homosapiens/MEX/2016/mex24 (GenBank: MF801402). The cloned ZIKV E protein has a 99.85% nucleotide identity, and 100% amino acid identity with the ZIKV E protein of the Brazilian strain (Paraiba 2015; GenBank: KY558989.1), a strain directly related to cases of microcephaly in Brazil [55, 56]. An empty pcDNA 3.0 plasmid was used as a transfection control (EMPTY).

Bacteria of the STBL3 strains were transformed with the E-ZIKA plasmid that was cloned into the pcDNA 3.0 vector and grown in 200 mL Luria-Bertani broth medium, the procedure was similar to the EMPTY vector. The cultures were incubated overnight at 37 °C and 150 rpm. To obtain purified DNA plasmids, the Pure LinkTM HiPure Plasmid Filter Maxiprep Kit (Invitrogen, cat# K210017) was used according to the manufacturer's instructions. Subsequently, the purified DNA was quantified using a NanoDrop One Microvolume UV-Vis Spectrophotometer (Thermo Fisher Scientific Inc, cat: ND-ONE) following the manufacturer's instructions. The DNA was stored at −20 °C until further use.

2.3. Cell transfections

To optimize the expression of the protein of interest, a DNA transfection curve was constructed, using 4.5×10^5 HEK-293T cells seeded in 6-well plates with 0.5, 1, 2, 3, 4, and 5 µg of the E-ZIKA plasmid. In U-87 MG cells, 2, 3, and 4 µg of the E-ZIKA plasmid at 48 hours (h) or 3 and 4 µg for 72 h were used. Subsequently, 2 µg of DNA was used for all the experiments. Non-transfected cells were used as the negative control (NEG or NEGATIVE). Transfections were performed using Lipofectamine 3000 (Invitrogen, cat# L3000-015) with a Lipofectamine/DNA ratio of 2:1 according to the manufacturer's instructions. After 48 h of incubation, cells were processed for analysis.

2.4. Protein extraction

After 48-72 h of incubation, cells were lysed with 60 µL of lysis buffer (50mM Tris-Cl pH 8.0, 1mM EDTA, 0.5% NP40, 0.5% Triton 150mM NaCl), supplemented with Complete Protease Inhibitor (Roche, cat# 11697498001). The Pierce BCA Protein Assay Kit (Thermo Fisher Scientific Inc, cat# 23223) was used for the quantification of proteins from the cell extracts in the spectrophotometer iMark Microplate Reader (Bio-Rad). Samples were stored at − 20 °C until use.

2.5. Immunoblotting assays

For western blot analysis, Brefeldin A (BFA) (Sigma-Aldrich, cat# B7651) was used as a positive control to induce UPR and was administered for 24 h (3µg/mL) to cells. After protein quantification of the treated cell cultures, 50 µg of protein was loaded onto 12% and 15% polyacrylamide gels for the detection of the proteins of interest. After electrophoresis, proteins were transferred onto PVDF membranes (Bio-Rad, cat# 1620177) and blocked with 5% skim milk. The following primary antibodies were used: anti-ZIKV E protein (1:1000, GeneTex, cat# GTX133314), anti-GRP78 (1:1000, R&D Systems, cat# MAB4846), anti-calreticulin (1:1000, Santa Cruz Biotechnology, cat# sc-373863), anti-caspase 3 (1:200, Cell Signaling Technology, cat# 9662), and anti-LC3B (1:1000, GeneTex, cat# GTX82986). Membranes were incubated overnight at 4 °C and then with an anti-β-actin HRP conjugated (1:40000, Sigma Aldrich, cat# A3854) for 20 minutes. The next day, membranes were washed using Tris Buffered Saline with Tween (0.1%) 1X buffer (TBST) and incubated with the secondary antibodies: anti-mouse HRP (1:2000, Invitrogen, cat# 62-6520), or anti-rabbit HRP (1:2000, Invitrogen, cat# 65-6120) for one hour. The membranes were then washed and developed with Western Lightning Plus-ECL (PerkinElmer, Inc, cat# NEL104001EA), following the manufacturer's instructions. The membranes were photo-documented using the FUSION SOLO S (Vilver) instrument, and densitometry analysis was performed using the ImageJ® Software (NIH). A buffer stripping containing, Tris-HCl 62.5 mM pH 6.8, mercaptoethanol 100mM, SDS 2% w/v, was used for stripping and detection of different proteins on the same membrane.

2.6. Immunofluorescence

To determine the presence of intracellular cellular and viral proteins, cells were fixed and permeabilized, while non-permeabilized cells were used for the detection of cell membrane proteins. Subsequently, cells were washed between each step with phosphate-buffered saline (PBS), and 1% Bovine Serum Albumin IgG-Free (BSA) (Jackson ImmunoResearch, cat# 001-000-162) blocking solution was added for 1 h at room temperature. After blocking, primary antibodies against the proteins of interest were added overnight at 4 °C. For the detection of cytoplasmic and ER proteins, 4% paraformaldehyde and 0.2% Triton X-100 were used to fix and permeabilize the cells. Later, cells were incubated with the following primary antibodies: anti-14-3-3 (1:100, Abcam, cat# ab14121-250) and anti-ZIKV E protein (1:300, GeneTex, cat# GTX133314) for cytoplasmic detection, or anti-GRP78 Alexa 488 conjugated (1:200, Thermo Fisher Scientific, cat# AF488 C38), and anti-calreticulin (1:200, Santa Cruz Biotechnology, cat# sc-373863) for ER detection. For β-actin and ZIKV E protein co-detection, methanol-acetone was used to fix, and 0.2% Triton X-100 was used to permeabilize the cells. Cells were then incubated with the following primary antibodies: anti-β-actin (1:100, Invitrogen, #MA5-15739) and anti-ZIKV E protein (1:300, GeneTex, cat# GTX133314).

For the detection of cell membrane proteins, 4% paraformaldehyde was used as a fixative and no permeabilization step was performed. The cells were then incubated with primary antibodies against anti-β-catenin (1:100, Invitrogen, cat# 138400) and anti-ZIKV E protein (1:300, GeneTex, cat# GTX133314).

The next day, cells were washed with PBS, and secondary antibodies were subsequently added, depending on

the combination of antibodies and their origin. ALEXA FITC 488 (Invitrogen, cat# A11001) and ALEXA TRITC 594 (Invitrogen, cat# A21203) were used for anti-mouse detection. ALEXA FITC 488 (Invitrogen, cat# A11008) and ALEXA 555 (Invitrogen, cat# A21428) were used for anti-rabbit detection, and cells were incubated for one hour at room temperature. Subsequently, cells were washed and mounted with Vectashield with DAPI (Vector laboratories, cat# H-1200) on slides for subsequent analysis using a Leica TCS SP8 laser confocal microscope with a Leica HC PL APO CS2 63x/1.40 oil objective with a pinhole size of 1 AU, smart offset of 0.2%, and pixel dwell time of 600 ns. The images were processed using ImageJ® software (NIH) and analyzed using the Pearson correlation coefficient and line scan methods, which measure the relative fluorescence using the linear trace of an arrow through the distance in the different channels.

2.7. Trypan blue assay

After treatment, cells were washed with PBS, and trypsinized. Subsequently, 10 µL of the cell sample was added and resuspended in 90 µL of trypan blue, mixed gently, and 10 µL of the suspension was poured into a Neubauer chamber (MarienFeld, cat# 0610030) in duplicate. Unstained cells represent live cells, and dead stained cells were expressed as a percentage of the total cell number.

2.8. Statistical analysis

Statistical analyses were performed with the GraphPad Prism Version 8.0.2 software (263) and IBM SPSS version 25. All samples were tested for normality (Shapiro-Wilk test, $p \leq 0.05$); additionally, those samples used for the ANOVA-test, passed the test of equality of variances (Levene´s test, $p \geq 0.05$). Later the one-way ANOVA test, two-way ANOVA test, unpaired t-test, and Tukey's *post-hoc* analysis (for parametric samples), were performed. For non-parametric analysis, the Kruskal-Wallis and the Dunn´s *post-hoc* analysis multiple comparisons tests were employed. p values ≤ 0.05 were considered statistically significant. All experiments were independently performed in triplicate.

3. Results

3.1. The ZIKV E protein is efficiently expressed in transfected cells

A DNA concentration curve was generated in HEK-293T cells to determine the optimal concentration to transfect the E-ZIKA plasmid vector. The results showed a high expression of the ZIKV E protein using 2, 3, or 4 µg of plasmid, as determined by western blot analysis (Fig.1 a). To optimize the expression of ZIKV E protein in U-87 MG cells, they were transfected with 2, 3, and 4 µg of DNA, and incubated for a period of 48 h; in addition, 3 and 4 µg were also used with an incubation time of 72 h. 2 µg of DNA was used for immunofluorescence and the subsequent experiments in both cell lines (Fig. 1b and S1 Fig.).

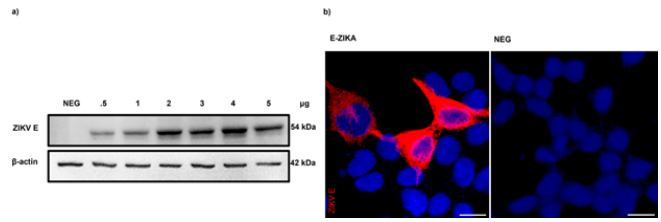

Fig. 1. Characterization of the expression ZIKV E protein in transfected cells. a) Western blot analysis of ZIKV E protein with different concentrations of DNA and untreated cells as a negative control (NEG). b) Immunofluorescence against ZIKV E protein (red) represents transfection with 2 µg of plasmid; DAPI (blue). Non-transfected cells (NEG) were used as control. Scale bar 15 µm

3.2. Expression of the ZIKV E protein does not cause cell death

After observing that the ZIKV E protein was expressed in transfected cells, we performed a cell viability assay to detect whether the expression of the ZIKV E protein induced the death of HEK-293T cells. Cells were collected at different times after transfection with 2 µg of plasmid or treatment with BFA (a fungal metabolite that in mammalian cells blocks vesicular transport of the ER-Golgi system [57], stimulating cellular stress and activating the UPR [58]) and stained with trypan blue. The data show that only cells treated with BFA presented a significant decrease in cell viability after treatment, compared with the cells transfected with the ZIKV E protein-encoding plasmid. Indeed, no differences in cell viability were observed among the cells transfected with the ZIKV E protein plasmid, the EMPTY plasmid, cells treated with LIPOFECTAMINE alone, or cells without treatment (NEG) at any time post-transfection, (Fig. 2). Therefore, these results indicate that the expression of ZIKV E protein does not cause cell death.

3.3. Expression of the ZIKV E protein does not induce an ER stress response

Since the ZIKV E protein interacts with GRP78 during viral infections and UPR response is triggered in infected cells [40, 51, 52], we next examined whether the expression of the ZIKV E protein alone, without the context of a viral infection, was capable of inducing this type of response. To do this, the levels of GRP78 were analyzed in transfected cells expressing the ZIKV E protein, using BFA as a positive control. Cells underwent different treatments and the levels of GRP78 as a marker of the UPR, and calreticulin (CRT) as an ER resident control protein, [59–61] were determined by western blot analysis. All data were normalized to β-actin as a loading control (Fig. 3a). The results indicated that the expression of the ZIKV E protein

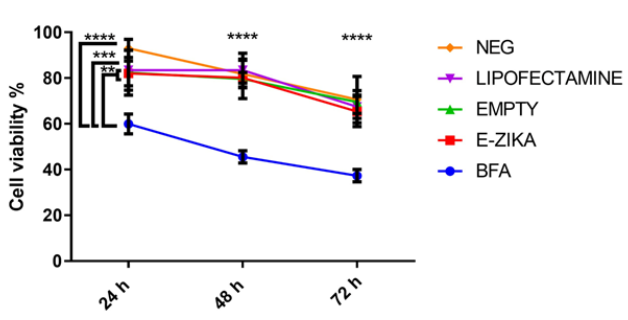

Fig. 2. Analysis of cell viability over time using trypan blue. a) BFA versus E-ZIKA, and EMPTY to 24 h *(**$p \leq 0.01$)*. b) BFA versus LIPOFECTAMINE to 24 h *(***$p \leq 0.005$)*. c) BFA versus NEG to 24 h and E-ZIKA, EMPTY, LIPOFECTAMINE, and NEG to 48 and 72 h *(****$p \leq 0.001$)*. Shapiro-Wilk test for normality, two-way ANOVA, and Tukey's *post-hoc* were performed.

alone did not induce GRP78 or CRT overexpression, while a clear increase in the expression of GRP78 was observed only in BFA treated cells (Fig. 3b). No significant changes in the expression of CRT were observed with any treatment (Fig. 3c).

Once it was confirmed that the UPR was not activated, we decided to analyze whether the ZIKV E protein activated cell death by caspase 3. These results show that there was no release of the 17 kDa cleaved caspase 3 (the active form) in cells expressing ZIKV E protein. These results suggest that ZIKV E protein does not activate the apoptotic cell death pathway (Fig. 3d). Finally, LC3-II was determined and used as an indicator of autophagy. The results showed significant activation of autophagy only in cells treated with BFA in comparison with untreated cells [62, 63]. However, no significant autophagy activation was observed in cells transfected with plasmids ZIKA E or EMPTY, or treated with LIPOFECTAMINE (LP) alone. These results indicate that the expression of the ZIKV E protein alone does not result in activation of the UPR response, or the apoptosis or autophagy pathways (Fig. 3a, e). Of note, similar results indicated no UPR was induced in the U-87 MG glioma cells expressing recombinant ZIKV E, even though these cells readily responded when treated with BFA (S2 Fig.).

3.4. ZIKV E protein targets the ER

After observing that the expression of the ZIKV E protein did not affect cellular homeostasis, we decided to analyze the subcellular localization of this protein. To this end, co-detection of ZIKV E protein with the ER-resident chaperone CRT was performed by immunofluorescence in cells undergoing the different treatments (Fig. 4a). Pearson's correlation coefficient analysis indicated a strong co-localization of ZIKV E and CRT (Fig. 4b). To complement these results, line scan analysis was performed. These data corroborate the subcellular localization of the ZIKV E protein in the ER, showing that the relative fluorescence units (RFU) of ZIKV E expression throughout the cell overlap with CRT (Fig. 4c). Only the CRT signal was observed in non-transfected cells used as control (Fig. 4d).

We subsequently analyzed whether there was co-localization of the ZIKV E protein with GRP78, given that no changes in GRP78 expression were observed by western blot analysis (Fig. 5a). The Pearson's correlation coefficient analysis showed a significant difference between E-ZIKA transfected and non-transfected cells (Fig. 5b). Line scan analysis was also performed to corroborate these data. The results showed an expression pattern for ZIKV E protein similar to that of GRP78. Only the signal for GRP78 was observed in non-transfected cells, used as negative controls (Fig. 5c, d). These data suggest that like in infected cells, the recombinant ZIKV E protein is located in the ER, and feasibly interacts with GRP78.

3.5. The ZIKV E protein is found in the cytoplasm

To better characterize the intracellular location of the recombinant ZIKV E protein, its presence in the cytoplasm was also analyzed. To do this, immunofluorescence was performed in cells transfected with the plasmid, and co-detection of ZIKV E protein (red) and 14-3-3 (green), a regulatory protein that binds to different signaling proteins, present mainly in the cytoplasm was performed [64]. These analyses were carried out in the basal sections of the cell, as this is where we found the cytoplasm to be the most extended. A Pearson's correlation coefficient of 0.356 was obtained, suggesting that some fraction of the recombinant ZIKV E protein may reach the cytoplasm and co-localize with 14-3-3 proteins (Fig. 6a, b). Line scan analysis

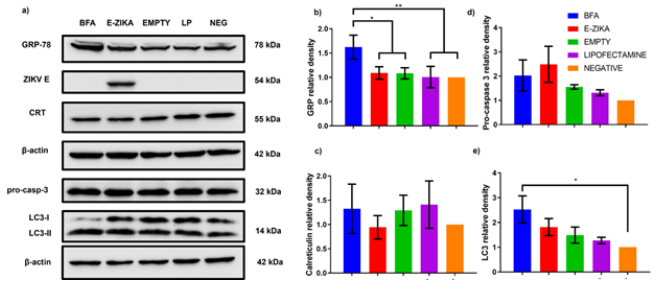

Fig. 3. Detection of UPR biomarkers. a) Representative western blot analysis of the biomarkers of interest. b) Relative expression of GRP78 protein is dependent on the treatment of interest. BFA showed a significant difference compared with the other treatments. c) Relative CRT expression under different treatments of interest. CRT showed no significant differences concerning treatment. d) Relative expression of pro-caspase 3 (because there was no cleavage of caspase 3 in any of the treatments of interest). There was no significant difference in the accumulation of inactive caspase (pro-caspase 3). e) Relative expression of LC3-II. The cells treated with BFA showed a significant difference compared to the untreated cells (NEGATIVE). β-actin expression was used as a reference. Shapiro-Wilk test for normality, One-way ANOVA (and non-parametric or mixed), Dunn´s multiple comparisons test for LC3-II and Tukey's post hoc analysis for GRP78, pro-caspase 3 and CRT were performed. $*p \leq 0.05$, $**p \leq 0.01$. Results of at least 3 independent experiments are shown. Densitometry analysis was performed using the ImageJ® Software (NIH), and normalized concerning β-actin.

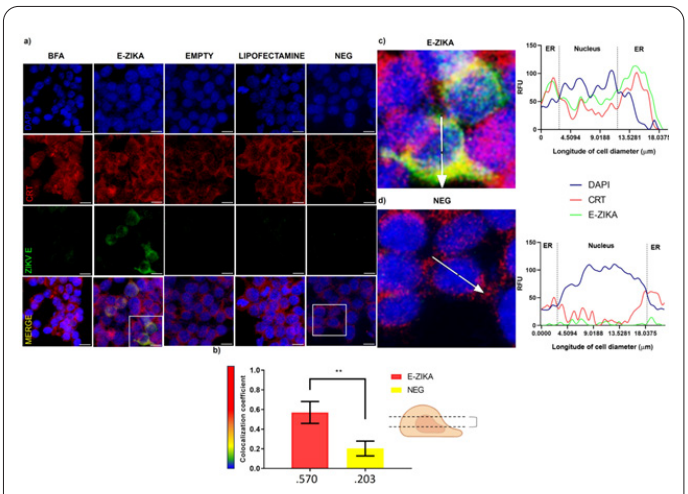

Fig. 4. Subcellular localization of ZIKV E protein in the ER. a) Immunofluorescence for the co-detection of ZIKV E protein (green) and the CRT chaperone (red) under different cellular conditions. Nuclei were stained blue (DAPI). b) Pearson correlation coefficient for ZIKV E protein colocalization versus CRT. Shapiro-Wilk test for normality and Unpaired t-tests were used. $**p \leq 0.01$. c) Line scan analysis of the subcellular location of the ZIKV E protein and CRT. d) Line scan analysis of negative control. The plotted line indicates the longitudinal diameter of the cell in the magnified image (white arrow). The RFUs from each of the individual channels were measured using the ImageJ® software (NIH). Immunofluorescence was performed using confocal microscopy, and a projection of the medial part of the cells was performed as indicated in the images. Scale bar 15 µm.

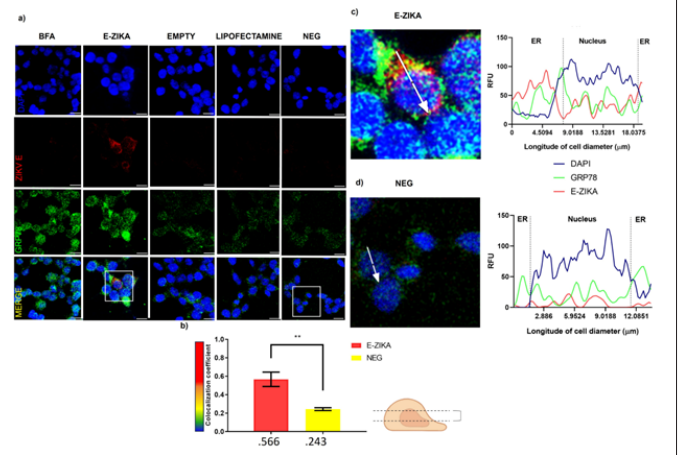

Fig. 5. Co-localization of ZIKV E protein and GRP78. a) Immunofluorescence for the co-detection of ZIKV E protein (red) and GRP78 (green) under different cellular conditions. Nuclei were stained with blue (DAPI). b) Pearson's correlation coefficient for the colocalization of ZIKV E versus GRP78. Unpaired t-tests were used. *$p \leq 0.05$. c) Line scan analysis of subcellular localization of ZIKV E versus GRP78. d) Line scan analysis of negative control. The plotted line indicates the longitudinal diameter of the cell in the magnified image (white arrow). The RFUs from each of the individual channels were measured using the ImageJ® software (NIH). Immunofluorescence was performed using confocal microscopy, and a projection of the medial part of the cells was performed as indicated in the images. Scale bar 15 μm.

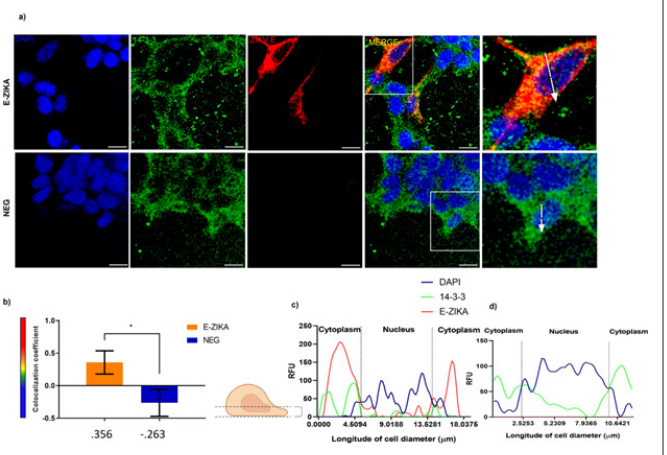

Fig. 6. Subcellular localization of ZIKV E protein in the cytoplasm with 14-3-3 protein. a) Immunofluorescence analysis for the co-detection of ZIKV E protein (red) and the 14-3-3 protein (green); nuclei are shown in blue (DAPI). b) Pearson's correlation coefficient between transfected and non-transfected cells. Shapiro-Wilk test for normality and Unpaired t-tests were used. *$p \leq 0.05$. c) Line scan analysis of the subcellular localization of ZIKV E protein versus 14-3-3 protein. d) Line scan analysis of negative control. The plotted line indicates the longitudinal diameter of the cell in the magnified image (white arrow). The RFUs from each of the individual channels were measured using the ImageJ® software (NIH). Immunofluorescence was performed using confocal microscopy, and a projection of the basal part of the cells was performed as indicated in the images. Scale bar 15 μm.

corroborated these results, showing higher RFUs in the cytoplasm for both proteins. Non -transfected cells used as control showed only a 14-3-3 signal (Fig. 6c, d). During ZIKV infection, the ZIKV E protein is mainly found inside the lumen of the ER, and presumably none in the cytoplasm [20–22]; however, it seems that a small fraction of the recombinant ZIKV E protein reaches the cytoplasm.

To confirm the cytoplasmic presence of the recombinant ZIKV E protein, immunofluorescence for ZIKV E protein (red) and β-actin (green), also a cytoplasm protein was performed [65] (Fig. 7a). Similar to 14-3-3, the ZIKV E protein showed a moderate Pearson correlation coefficient of 0.413 with β-actin, with a significant difference compared to no-transfected cells, which only showed signal for actin (Fig. 7b). Line scan analysis revealed a relationship between the RFUs of each protein in the cytoplasm (Fig. 7c, d). These data corroborate the presence of the recombinant ZIKV E protein in the cytosol of transfected cells.

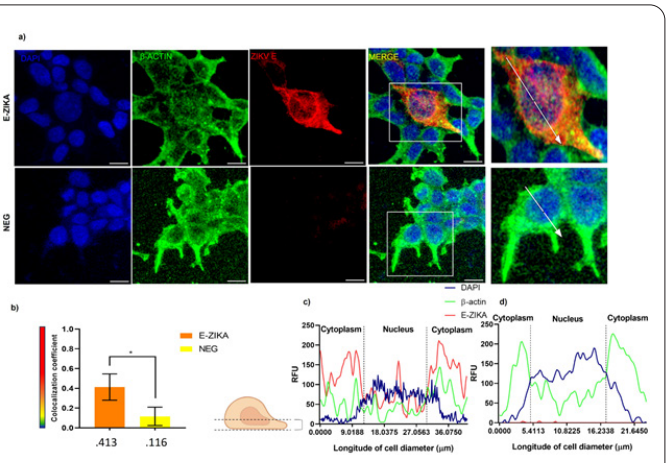

Fig. 7. Subcellular localization of ZIKV E protein in the cytoplasm with β-actin protein. a) Immunofluorescence analysis for the co-detection of ZIKV E protein (red) and β-actin protein (green), nuclei are shown in blue (DAPI). b) Pearson's correlation coefficient between transfected and non-transfected cells. Unpaired t-tests were used. *$p \leq 0.05$. c) Line scan analysis of the subcellular localization of ZIKV E protein versus β-actin. d) Line scan analysis of negative control. The plotted line indicates the longitudinal diameter of the cell in the magnified image (white arrow). The RFUs from each of the individual channels were measured using the ImageJ® software (NIH). Immunofluorescence was performed using confocal microscopy, and a projection of the basal part of the cells was performed as indicated in the images. Scale bar 15 μm.

3.6. The ZIKV E protein is expressed on the cell plasma membrane

Once we observed that ZIKV E protein was found in the ER lumen and the cytoplasm of transfected cells, we performed immunofluorescence assays to determine whether it could be transported to the cell membrane. For this purpose, the co-detection of ZIKV E protein with β-catenin, a fundamental protein in the dynamics of the cytoskeleton and cell membrane [66] was carried out using non-permeabilized cells. Pearson's correlation coefficient was used to detect the level of co-localization on the cell membrane. Interestingly, in the transfected non-permeabilized cells, a strong co-localization of the ZIKV E protein and β-catenin was observed (Fig. 8a), with a significant difference about the non-transfected cells (Fig. 8b). The results were corroborated by line scan analysis, which demonstrated an RFU for both proteins in the plasma membrane (Fig. 8c, d). These experiments thus demonstrate that the recombinant ZIKV E protein is transported to the plasma membrane.

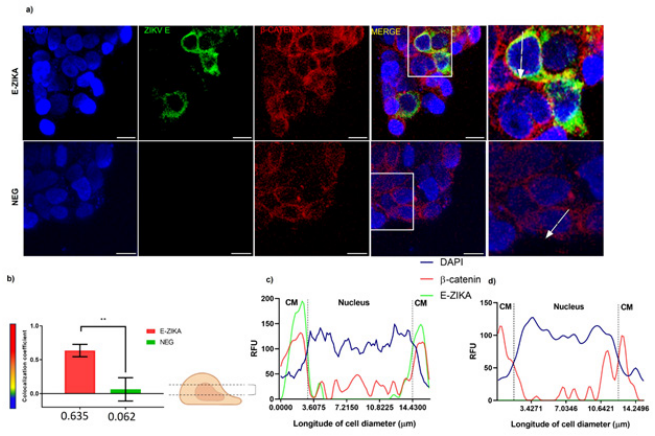

Fig. 8. Subcellular localization of ZIKV E protein in the cell membrane. a) Immunofluorescence analysis for the co-detection of ZIKV E protein (green) and β-catenin protein (red); nuclei are shown in blue (DAPI). b) Pearson's correlation coefficient between transfected and non-transfected cells. Shapiro-Wilk test for normality and Unpaired t-tests were used. $**p \leq 0.01$. c) Line scan analysis of the subcellular localization of ZIKV E protein versus β-catenin protein. d) Line scan analysis of negative control. The plotted line indicates the longitudinal diameter of the cell in the magnified image (white arrow). The RFUs from each of the individual channels were measured using the ImageJ® software (NIH). Scale bar 15 µm.

4. Discussion

The tropism of the ZIKV to neural stem cells is due to the ZIKV E protein [8]. The virus also presents tropism for glioblastoma stem cells [67] which possess specific receptors such as integrin αvβ5 that allow virion attachment and entry causing cell death [28, 68]. During ZIKV infection in these cells, a single-stranded RNA encoding a polyprotein that contains three structural proteins, the capsid protein (outside the ER), while prM and E, as well as non-structural proteins (NS1, NS2A, NS2B, NS3, NS4A, NS4B and NS5), are directed to the ER by the signal peptide, which is located downstream of the capsid sequence [21]. ER targeting allows the formation and assembly of viral particles after genome synthesis in replication loops [69, 70].

Due to the importance of the ZIKV E protein in cellular tropism, and its potential use in cell targeting of neural cells, we decided to explore the potential role of the ZIKV E protein *per se* in cellular physiology once it is expressed in the cell without the context of other viral proteins. The HEK-293T cell line was used because it is easily transfected (Fig. 1), and it is also widely used for the manufacture of gene and cell therapy products [71–74]; moreover, it shows some neuronal characteristics [75, 76]. Furthermore, since the ZIKV has a tropism for neural stem cells and glioma cells, we confirmed that ZIKV E protein does not induce the UPR in U-87 MG human glioma cells (S2 Fig.), thus suggesting that regardless of the cell type the protein by itself, does not instigate the UPR, nor apoptosis, as assessed by caspase 3 activity.

We first analyzed HEK-293T cell viability demonstrating that the ZIKV E protein does not induce the death of transfected cells (Fig. 2). These results coincide with a previous report, showing that the expression of the ZIKV E protein, in the absence of other viral proteins, did not induce cell death [38]. Thus no decreases in cell viability were found after the expression of the ZIKV E, whereas during viral infection, the expression of the complete viral genome triggers the death of neural cells leading to microcephaly [18, 40, 77].

Our results, after analyzing by western blot whether ZIKV E protein can activate biomarkers of cellular homeostasis, such as the UPR, and rescue pathways such as autophagy and apoptotic cell death, show that the ZIKV E protein does not activate the UPR, because there is no increase in the expression of GRP78 and CRT, compared to controls (Fig. 3a, b, c and S2 Fig.). Moreover, we observed that ZIKV E protein does not induce apoptosis (Fig. 3d and S2 Fig.). Flaviviruses can induce NS4A-dependent autophagy [78], however, we did not observe that the expression of the ZIKV E protein by itself induced autophagy (Fig. 3e and S2 Fig.). Interestingly, our results indicate that the ZIKV E protein without a signal sequence can be directed to the cell membrane passing through the ER. Thus our data show that the ZIKV E protein does not require the amino-terminal signal sequence [21] because, despite its absence, it can target the ER, as demonstrated by its co-localization with CRT, a resident chaperone of this organelle (Fig. 4a, b, c). Other studies have shown that certain proteins can be inserted into the ER, post-translationally, by a hydrophobic sequence near the carboxyl-terminal tail [79, 80], similar to that of the ZIKV E protein [81].

Furthermore, ZIKV induces the activation of the UPR to enhance viral replication, increasing the activity of UPR genes such as p-PKR, p-eIF2α, and IRE1/XBP1s and arrests protein synthesis by a mechanism dependent on non-structural genes such as NS3 and NS4A [38]. In dengue virus (DENV) infections, E, NS1, NS2A, NS2B, and NS4B proteins induce the activation of XBP1, relieving ER stress through the ERAD pathway, but also inhibit mediators of apoptosis, allowing survival and cellular and viral replication [82]. However, there are no reports that demonstrate that the ZIKV E protein induces any of these effects. It has been reported that ZIKV E protein interacts with GRP78 [51, 52], nevertheless, there are contradictory reports regarding the alteration in the expression of GRP78 in cells infected with ZIKV, since some reports indicated overexpression [51], while other its downregulation [83]. Interestingly, there are, to the best of our knowledge, no reports of the effect on GRP78 expression induced by the ZIKV E protein. Therefore, in this work, we show that the ZIKV E protein does not affect the levels of GRP78 (Fig. 3b, 5a). However, we observed that there is co-localization of the ZIKV E and GRP78 in the ER, which is consistent with interaction studies in the literature (Fig. 5b, c). GRP78 overexpression induces the inhibition of protein synthesis. Yet, our results indirectly coincide with the study by Hou and collaborators where they observed that the expression of ZIKV E protein by itself did not inhibit protein synthesis [38].

Since during ZIKV infection, the ZIKV E protein is directed to the ER by the signal sequence of the polyprotein [21, 84], we asked whether the ZIKV E protein *per se* could be found in the cytoplasm, and our results showed low levels of co-localization with the 14-3-3 protein and β-actin. However, Pearson´s correlation analysis indicated that the levels of expression of the ZIKV E protein are lower in cytoplasm when compared with the ER, suggesting that once the protein is synthesized it is quickly directed to the ER (Figs. 6 and 7).

After observing that the ZIKV E protein is in the cytoplasm and that it is directed to the ER, we analyzed whether it was found in the cell membrane. In the non-permeabilized cells, a signal for β-catenin was not expected, since this protein is located in the inner side of the membrane, and expected to exclusively detect the ZIKV E protein. However, both proteins were detected in this condition in the immunofluorescence assays. Previously it has been shown that the use of aldehydes as fixatives can semi-permeabilize the cell membrane [85]; therefore, the antibody may partially cross the cell membrane [86]. These results demonstrate the localization of the ZIKV E in the plasma membrane (Fig. 8); however, more studies will be needed to determine the precise localization of ZIKV E protein due to its transmembrane domain. Elucidation of the traffic route used for the ZIKV E protein to reach the plasma membrane requires further studies, but most likely involves the constitutive secretion pathway via the Golgi complex, as has been observed for mature virions during infection [20–22].

5. Conclusion

The present results demonstrate that the ZIKV E protein reaches the cell membrane, passing through the ER, without causing activation of the UPR or cell death, making the expression of ZIKV E protein alone a promising tool to guide therapeutic vectors to gliomas. However, the expression of this viral protein on the vector surface may nonetheless represent an obstacle to the use of recombinant ZIKV E protein as a glioma stem cell-targeting molecule, because of the possible presence of memory cells or antibodies against the virus, induced by past ZIKV infections [87]. Understanding the pathway by which the ZIKV E protein is processed in the HEK-293T and other cell lines that serve as a platform for the production of pseudotyped viral particles or cell therapy, could allow us to develop new and safer biotechnological approaches for the treatment of gliomas [29, 88, 89], and other types of diseases [90]. Or the production of different vectors, for gene therapy, or even to generate safer and more effective recombinant proteins (54) and vaccines [89, 91, 92].

Acknowledgments

We thank Dr. L. Cedillo-Barrón, (Cinvestav), Dr. R. Valles-Ríos, (División de Investigación. Facultad de Medicina de la UNAM), Dr. R.M del Ángel Núñez de Cáceres, (Cinvestav), and Dr. L. González-Mariscal, (Cinvestav), for the donation of antibodies and reagents, and technical advice; Paula Vergara and Araceli Navarrete for technical support. DHMP received a scholarship from CONAHCYT.

Conflict of interests

The author has no conflicts with any step of the article preparation.

Consent for publications

The author read and approved the final manuscript for publication.

Ethics approval and consent to participate

No humans or animals were used in the present research.

Informed consent

The authors declare that no patients were used in this study.

Availability of data and material

The data that support the findings of this study are available from the corresponding author upon reasonable request

Authors' contributions

Conceptualization: David Hernán Martínez-Puente, María de Jesús Loera-Arias, Juan E Ludert, José Segovia.
Data curation: José Segovia, Juan E Ludert, María de Jesús Loera-Arias.
Formal analysis: David Hernán Martínez-Puente, José Segovia.
Funding acquisition: José Segovia, Juan E. Ludert.
Investigation: David Hernán Martínez-Puente, Manuel Lara-Lozano, Nicolás Aguirre-Pineda.
Methodology: David Hernán Martínez-Puente, Juan E. Ludert, José Segovia.
Project administration: José Segovia, Juan E. Ludert
Resources: Juan E. Ludert**,** José Segovia.
Supervision: José Segovia.
Validation: José Segovia.
Writing – original draft: David Hernán Martínez-Puente, José Segovia.

Funding

This work was partially funded by Cinvestav (JS); CONAHCYT-Mexico (PRONAII 302979 A-1-S-9005 to JEL).

References

1. Dick GWA, Kitchen SF, Haddow AJ (1952) Zika Virus (I). Isolations and serological specificity. Transactions of the Royal Society of Tropical Medicine and Hygiene 46:509–520. https://doi.org/10.1016/0035-9203(52)90042-4
2. Peiter PC, Pereira R dos S, Nunes Moreira MC, et al (2020) Zika epidemic and microcephaly in Brazil: Challenges for access to health care and promotion in three epidemic areas. PLoS One 15:e0235010. https://doi.org/10.1371/journal.pone.0235010
3. Li C, Xu D, Ye Q, et al (2016) Zika Virus Disrupts Neural Progenitor Development and Leads to Microcephaly in Mice. Cell Stem Cell 19:672. https://doi.org/10.1016/j.stem.2016.10.017
4. Schmitt K, Curlin JZ, Remling-Mulder L, et al (2023) Zika virus induced microcephaly and aberrant hematopoietic cell differentiation modeled in novel neonatal humanized mice. Front Immunol 14:1060959. https://doi.org/10.3389/fimmu.2023.1060959
5. Muthuraj PG, Sahoo PK, Kraus M, et al (2021) Zika virus infection induces endoplasmic reticulum stress and apoptosis in placental trophoblasts. Cell Death Discov 7:24. https://doi.org/10.1038/s41420-020-00379-8
6. Mufrrih M, Chen B, Chan S-W (2021) Zika Virus Induces an Atypical Tripartite Unfolded Protein Response with Sustained Sensor and Transient Effector Activation and a Blunted BiP Response. mSphere 6:e0036121. https://doi.org/10.1128/mSphere.00361-21
7. Francipane MG, Douradinha B, Chinnici CM, et al (2021) Zika Virus: A New Therapeutic Candidate for Glioblastoma Treatment. Int J Mol Sci 22:10996. https://doi.org/10.3390/ijms222010996
8. Annamalai AS, Pattnaik A, Sahoo BR, et al (2017) Zika Virus Encoding Nonglycosylated Envelope Protein Is Attenuated and Defective in Neuroinvasion. J Virol 91:e01348-17. https://doi.org/10.1128/JVI.01348-17
9. Carbaugh DL, Baric RS, Lazear HM (2019) Envelope Protein Glycosylation Mediates Zika Virus Pathogenesis. J Virol 93:e00113-19. https://doi.org/10.1128/JVI.00113-19
10. Ryu W-S (2017) Chapter 12 - Flaviviruses. In: Ryu W-S (ed) Mo-

lecular Virology of Human Pathogenic Viruses. Academic Press, Boston, pp 165–175
11. Sikka V, Chattu VK, Popli RK, et al (2016) The emergence of zika virus as a global health security threat: A review and a consensus statement of the INDUSEM Joint working Group (JWG). Journal of Global Infectious Diseases 8:3. https://doi.org/10.4103/0974-777X.176140
12. Grard G, Caron M, Mombo IM, et al (2014) Zika Virus in Gabon (Central Africa) – 2007: A New Threat from Aedes albopictus? PLoS Negl Trop Dis 8:. https://doi.org/10.1371/journal.pntd.0002681
13. RAGHUNATH P (2018) Does Zika Virus Really Causes Microcephaly in Children Whose Mothers Became Infected with the Virus during Their Pregnancy? Iran J Public Health 47:613–614
14. Musso D, Roche C, Robin E, et al (2015) Potential sexual transmission of Zika virus. Emerging Infect Dis 21:359–361. https://doi.org/10.3201/eid2102.141363
15. Rawal G, Yadav S, Kumar R (2016) Zika virus: An overview. J Family Med Prim Care 5:523–527. https://doi.org/10.4103/2249-4863.197256
16. Barbelanne M, Tsang WY (2014) Molecular and cellular basis of autosomal recessive primary microcephaly. Biomed Res Int 2014:547986. https://doi.org/10.1155/2014/547986
17. Wen Z, Song H, Ming G (2017) How does Zika virus cause microcephaly? Genes Dev 31:849–861. https://doi.org/10.1101/gad.298216.117
18. Cugola FR, Fernandes IR, Russo FB, et al (2016) The Brazilian Zika virus strain causes birth defects in experimental models. Nature 534:267–271. https://doi.org/10.1038/nature18296
19. Mysorekar IU, Diamond MS (2016) Modeling Zika Virus Infection in Pregnancy. New England Journal of Medicine 375:481–484. https://doi.org/10.1056/NEJMcibr1605445
20. Shi Y, Gao GF (2017) Structural Biology of the Zika Virus. Trends in Biochemical Sciences 42:443–456. https://doi.org/10.1016/j.tibs.2017.02.009
21. Sirohi D, Kuhn RJ (2017) Zika Virus Structure, Maturation, and Receptors. J Infect Dis 216:S935–S944. https://doi.org/10.1093/infdis/jix515
22. Wang A, Thurmond S, Islas L, et al (2017) Zika virus genome biology and molecular pathogenesis. Emerging Microbes & Infections 6:1–6. https://doi.org/10.1038/emi.2016.141
23. Zhang Y, Zhang W, Ogata S, et al (2004) Conformational changes of the flavivirus E glycoprotein. Structure 12:1607–1618. https://doi.org/10.1016/j.str.2004.06.019
24. Dai L, Song J, Lu X, et al (2016) Structures of the Zika Virus Envelope Protein and Its Complex with a Flavivirus Broadly Protective Antibody. Cell Host Microbe 19:696–704. https://doi.org/10.1016/j.chom.2016.04.013
25. Valente AP, Moraes AH Zika virus proteins at an atomic scale: how does structural biology help us to understand and develop vaccines and drugs against Zika virus infection? J Venom Anim Toxins Incl Trop Dis 25:. https://doi.org/10.1590/1678-9199-JVATITD-2019-0013
26. Watterson D, Kobe B, Young PR (2012) Residues in domain III of the dengue virus envelope glycoprotein involved in cell-surface glycosaminoglycan binding. J Gen Virol 93:72–82. https://doi.org/10.1099/vir.0.037317-0
27. Sapparapu G, Fernandez E, Kose N, et al (2016) Neutralizing human antibodies prevent Zika virus replication and fetal disease in mice. Nature 540:443–447. https://doi.org/10.1038/nature20564
28. Zhu Z, Mesci P, Bernatchez JA, et al (2020) Zika Virus Targets Glioblastoma Stem Cells through a SOX2-Integrin αvβ5 Axis. Cell stem cell 26:187-204.e10. https://doi.org/10.1016/j.stem.2019.11.016
29. Pöhlking C, Beier S, Formanski JP, et al (2023) Isolation of Cells from Glioblastoma Multiforme Grade 4 Tumors for Infection with Zika Virus prME and ME Pseudotyped HIV-1. International Journal of Molecular Sciences 24:4467. https://doi.org/10.3390/ijms24054467
30. Kumar A, Jovel J, Lopez-Orozco J, et al (2018) Human Sertoli cells support high levels of Zika virus replication and persistence. Sci Rep 8:5477. https://doi.org/10.1038/s41598-018-23899-x
31. Lee JK, Shin OS (2019) Advances in Zika Virus–Host Cell Interaction: Current Knowledge and Future Perspectives. Int J Mol Sci 20:. https://doi.org/10.3390/ijms20051101
32. Zwernik SD, Adams BH, Raymond DA, et al (2021) AXL receptor is required for Zika virus strain MR-766 infection in human glioblastoma cell lines. Mol Ther Oncolytics 23:447–457. https://doi.org/10.1016/j.omto.2021.11.001
33. Kaid C, Goulart E, Caires-Júnior LC, et al (2018) Zika Virus Selectively Kills Aggressive Human Embryonal CNS Tumor Cells In Vitro and In Vivo. Cancer Research 78:3363–3374. https://doi.org/10.1158/0008-5472.CAN-17-3201
34. Duvergé A, Negroni M (2020) Pseudotyping Lentiviral Vectors: When the Clothes Make the Virus. Viruses 12:1311. https://doi.org/10.3390/v12111311
35. Cronin J, Zhang X-Y, Reiser J (2005) Altering the Tropism of Lentiviral Vectors through Pseudotyping. Curr Gene Ther 5:387–398
36. Gutierrez-Guerrero A, Cosset F-L, Verhoeyen E (2020) Lentiviral Vector Pseudotypes: Precious Tools to Improve Gene Modification of Hematopoietic Cells for Research and Gene Therapy. Viruses 12:1016. https://doi.org/10.3390/v12091016
37. Mohd Ropidi MI, Khazali AS, Nor Rashid N, Yusof R (2020) Endoplasmic reticulum: a focal point of Zika virus infection. Journal of Biomedical Science 27:27. https://doi.org/10.1186/s12929-020-0618-6
38. Hou S, Kumar A, Xu Z, et al (2017) Zika Virus Hijacks Stress Granule Proteins and Modulates the Host Stress Response. Journal of Virology 91:e00474-17. https://doi.org/10.1128/JVI.00474-17
39. Emara MM, Brinton MA (2007) Interaction of TIA-1/TIAR with West Nile and dengue virus products in infected cells interferes with stress granule formation and processing body assembly. Proceedings of the National Academy of Sciences 104:9041–9046. https://doi.org/10.1073/pnas.0703348104
40. Alfano C, Gladwyn-Ng I, Couderc T, et al (2019) The Unfolded Protein Response: A Key Player in Zika Virus-Associated Congenital Microcephaly. Frontiers in Cellular Neuroscience 13:1–9. https://doi.org/10.3389/fncel.2019.00094
41. Wright MT, Plate L (2021) Revealing functional insights into ER proteostasis through proteomics and interactomics. Experimental Cell Research 399:112417. https://doi.org/10.1016/j.yexcr.2020.112417
42. Choi J-A, Song C-H (2020) Insights Into the Role of Endoplasmic Reticulum Stress in Infectious Diseases. Front Immunol 10:3147. https://doi.org/10.3389/fimmu.2019.03147
43. Almanza A, Carlesso A, Chintha C, et al (2019) Endoplasmic reticulum stress signalling – from basic mechanisms to clinical applications. The FEBS Journal 286:241–278. https://doi.org/10.1111/febs.14608
44. Guan B-J, Krokowski D, Majumder M, et al (2014) Translational Control during Endoplasmic Reticulum Stress beyond Phosphorylation of the Translation Initiation Factor eIF2α. J Biol Chem 289:12593–12611. https://doi.org/10.1074/jbc.M113.543215
45. Liu Z, Lv Y, Zhao N, et al (2015) Protein kinase R-like ER kinase and its role in endoplasmic reticulum stress-decided cell fate. Cell Death Dis 6:e1822–e1822. https://doi.org/10.1038/

cddis.2015.183
46. Kwon D, Koh J, Kim S, et al (2018) Overexpression of endoplasmic reticulum stress-related proteins, XBP1s and GRP78, predicts poor prognosis in pulmonary adenocarcinoma. Lung Cancer 122:131–137. https://doi.org/10.1016/j.lungcan.2018.06.005
47. Anderson CM, Macleod KF (2019) Chapter Five - Autophagy and cancer cell metabolism. In: Montrose DC, Galluzzi L (eds) International Review of Cell and Molecular Biology. Academic Press, pp 145–190
48. Kroeger H, Grimsey N, Paxman R, et al (2018) The unfolded protein response regulator ATF6 promotes mesodermal differentiation. Sci Signal 11:eaan5785. https://doi.org/10.1126/scisignal.aan5785
49. Yang H, Niemeijer M, van de Water B, Beltman JB (2020) ATF6 Is a Critical Determinant of CHOP Dynamics during the Unfolded Protein Response. iScience 23:100860. https://doi.org/10.1016/j.isci.2020.100860
50. Chipurupalli S, Samavedam U, Robinson N (2021) Crosstalk Between ER Stress, Autophagy and Inflammation. Frontiers in Medicine 8:
51. Khongwichit S, Sornjai W, Jitobaom K, et al (2021) A functional interaction between GRP78 and Zika virus E protein. Sci Rep 11:393. https://doi.org/10.1038/s41598-020-79803-z
52. Royle J, Ramírez-Santana C, Akpunarlieva S, et al (2020) Glucose-Regulated Protein 78 Interacts with Zika Virus Envelope Protein and Contributes to a Productive Infection. Viruses 12:524. https://doi.org/10.3390/v12050524
53. Pulix M, Lukashchuk V, Smith DC, Dickson AJ (2021) Molecular characterization of HEK293 cells as emerging versatile cell factories. Current Opinion in Biotechnology 71:18–24. https://doi.org/10.1016/j.copbio.2021.05.001
54. Lara-Lozano M, Flores de los Ángeles C, Pérez-Silva NB, et al (2023) Low-scale production and purification of a biologically active optimized form of the antitumor protein growth arrest specific 1 (GAS1) in a mammalian system for post-translational analysis. Biochemical Engineering Journal 193:108858. https://doi.org/10.1016/j.bej.2023.108858
55. Krow-Lucal ER, Andrade MR de, Cananéa JNA, et al (2018) Association and birth prevalence of microcephaly attributable to Zika virus infection among infants in Paraíba, Brazil, in 2015–16: a case-control study. The Lancet Child & Adolescent Health 2:205–213. https://doi.org/10.1016/S2352-4642(18)30020-8
56. Melo AS de O, Aguiar RS, Amorim MMR, et al (2016) Congenital Zika Virus Infection: Beyond Neonatal Microcephaly. JAMA Neurology 73:1407–1416. https://doi.org/10.1001/jamaneurol.2016.3720
57. Kano F, Sako Y, Tagaya M, et al (2000) Reconstitution of Brefeldin A–induced Golgi Tubulation and Fusion with the Endoplasmic Reticulum in Semi-Intact Chinese Hamster Ovary Cells. MBoC 11:3073–3087. https://doi.org/10.1091/mbc.11.9.3073
58. Menu P, Mayor A, Zhou R, et al (2012) ER stress activates the NLRP3 inflammasome via an UPR-independent pathway. Cell Death Dis 3:e261–e261. https://doi.org/10.1038/cddis.2011.132
59. Pieren M, Galli C, Denzel A, Molinari M (2005) The Use of Calnexin and Calreticulin by Cellular and Viral Glycoproteins*. Journal of Biological Chemistry 280:28265–28271. https://doi.org/10.1074/jbc.M501020200
60. Uvarov AV, Mesaeli N (2008) Enhanced ubiquitin-proteasome activity in calreticulin deficient cells: A compensatory mechanism for cell survival. Biochimica et Biophysica Acta (BBA) - Molecular Cell Research 1783:1237–1247. https://doi.org/10.1016/j.bbamcr.2008.03.004
61. Liu H, Bowes RC, Water B van de, et al (1997) Endoplasmic Reticulum Chaperones GRP78 and Calreticulin Prevent Oxidative Stress, Ca2+ Disturbances, and Cell Death in Renal Epithelial Cells *. Journal of Biological Chemistry 272:21751–21759. https://doi.org/10.1074/jbc.272.35.21751
62. Runwal G, Stamatakou E, Siddiqi FH, et al (2019) LC3-positive structures are prominent in autophagy-deficient cells. Sci Rep 9:10147. https://doi.org/10.1038/s41598-019-46657-z
63. Chen DL, Engle JT, Griffin EA, et al (2015) Imaging Caspase-3 Activation as a Marker of Apoptosis-Targeted Treatment Response in Cancer. Mol Imaging Biol 17:384–393. https://doi.org/10.1007/s11307-014-0802-8
64. Fu H, Subramanian RR, Masters SC (2000) 14-3-3 Proteins: Structure, Function, and Regulation. Annual Review of Pharmacology and Toxicology 40:617–647. https://doi.org/10.1146/annurev.pharmtox.40.1.617
65. Dugina VB, Shagieva GS, Kopnin PB (2022) Cytoplasmic Beta and Gamma Actin Isoforms Reorganization and Regulation in Tumor Cells in Culture and Tissue. Front Pharmacol 13:895703. https://doi.org/10.3389/fphar.2022.895703
66. Valenta T, Hausmann G, Basler K (2012) The many faces and functions of β-catenin. EMBO J 31:2714–2736. https://doi.org/10.1038/emboj.2012.150
67. Zhu Z, Gorman MJ, McKenzie LD, et al (2017) Zika virus has oncolytic activity against glioblastoma stem cells. J Exp Med 214:2843–2857. https://doi.org/10.1084/jem.20171093
68. Wang S, Zhang Q, Tiwari SK, et al (2020) Integrin αvβ5 Internalizes Zika Virus during Neural Stem Cells Infection and Provides a Promising Target for Antiviral Therapy. Cell Reports 30:969-983.e4. https://doi.org/10.1016/j.celrep.2019.11.020
69. Hasan SS, Sevvana M, Kuhn RJ, Rossmann MG (2018) Structural biology of Zika virus and other flaviviruses. Nature Structural & Molecular Biology 25:13–20. https://doi.org/10.1038/s41594-017-0010-8
70. Stiasny K, Heinz FX (2006) Flavivirus membrane fusion. J Gen Virol 87:2755–2766. https://doi.org/10.1099/vir.0.82210-0
71. Aydin H, Azimi FC, Cook JD, Lee JE (2012) A Convenient and General Expression Platform for the Production of Secreted Proteins from Human Cells. J Vis Exp 4041. https://doi.org/10.3791/4041
72. Tan E, Chin CSH, Lim ZFS, Ng SK (2021) HEK293 Cell Line as a Platform to Produce Recombinant Proteins and Viral Vectors. Front Bioeng Biotechnol 9:796991. https://doi.org/10.3389/fbioe.2021.796991
73. Ferreira CB, Sumner RP, Rodriguez-Plata MT, et al (2020) Lentiviral Vector Production Titer Is Not Limited in HEK293T by Induced Intracellular Innate Immunity. Molecular Therapy Methods & Clinical Development 17:209–219. https://doi.org/10.1016/j.omtm.2019.11.021
74. Perpiñá U, Herranz C, Martín-Ibáñez R, et al (2020) Cell Banking of HEK293T cell line for clinical-grade lentiviral particles manufacturing. transl med commun 5:1–13. https://doi.org/10.1186/s41231-020-00075-w
75. He B, Soderlund DM (2010) Human Embryonic Kidney (HEK293) Cells Express Endogenous Voltage-Gated Sodium Currents and Nav1.7 Sodium Channels. Neurosci Lett 469:268. https://doi.org/10.1016/j.neulet.2009.12.012
76. Chiang C-W, Shu W-C, Wan J, et al (2021) Recordings from neuron–HEK cell cocultures reveal the determinants of miniature excitatory postsynaptic currents. J Gen Physiol 153:e202012849. https://doi.org/10.1085/jgp.202012849
77. de Oliveira CS, de Matos HJ, Ramos FL de P, et al (2020) Risk of Zika virus-associated birth defects in congenital confirmed cases in the Brazilian Amazon. Rev Panam Salud Publica 44:e116. https://doi.org/10.26633/RPSP.2020.116
78. McLean JE, Wudzinska A, Datan E, et al (2011) Flavivirus

NS4A-induced autophagy protects cells against death and enhances virus replication. J Biol Chem 286:22147–22159. https://doi.org/10.1074/jbc.M110.192500

78. Johnson N, Powis K, High S (2013) Post-translational translocation into the endoplasmic reticulum. Biochimica et Biophysica Acta (BBA) - Molecular Cell Research 1833:2403–2409. https://doi.org/10.1016/j.bbamcr.2012.12.008
80. Sun S, Mariappan M (2020) C-terminal tail length guides insertion and assembly of membrane proteins. Journal of Biological Chemistry 295:15498–15510. https://doi.org/10.1074/jbc.RA120.012992
81. Stiasny K, Medits I, Roßbacher L, Heinz FX (2023) Impact of structural dynamics on biological functions of flaviviruses. The FEBS Journal 290:1973–1985. https://doi.org/10.1111/febs.16419
82. Viettri M, León FR, Zambrano JL, Ludert JE (2022) La replicación del virus del dengue induce respuestas de estrés en el retículo endoplasmático rugoso y en el aparato de Golgi, tanto en células de vertebrados como de invertebrados (mosquitos). Universitas Medica 63:1–11
83. Turpin J, Frumence E, Harrabi W, et al (2020) Zika virus subversion of chaperone GRP78/BiP expression in A549 cells during UPR activation. Biochimie 175:99–105. https://doi.org/10.1016/j.biochi.2020.05.011
84. Tan TY, Fibriansah G, Kostyuchenko VA, et al (2020) Capsid protein structure in Zika virus reveals the flavivirus assembly process. Nat Commun 11:895. https://doi.org/10.1038/s41467-020-14647-9
85. Cheng R, Zhang F, Li M, et al (2019) Influence of Fixation and Permeabilization on the Mass Density of Single Cells: A Surface Plasmon Resonance Imaging Study. Front Chem 7:588. https://doi.org/10.3389/fchem.2019.00588
86. Fulton KA, Briggman KL (2021) Permeabilization-free en bloc immunohistochemistry for correlative microscopy. eLife 10:e63392. https://doi.org/10.7554/eLife.63392
87. Chen X, Anderson LJ, Rostad CA, et al (2021) Development and optimization of a Zika virus antibody-dependent cell-mediated cytotoxicity (ADCC) assay. J Immunol Methods 488:112900. https://doi.org/10.1016/j.jim.2020.112900
88. Kretschmer M, Kadlubowska P, Hoffmann D, et al (2020) Zikavirus prME Envelope Pseudotyped Human Immunodeficiency Virus Type-1 as a Novel Tool for Glioblastoma-Directed Virotherapy. Cancers (Basel) 12:1000. https://doi.org/10.3390/cancers12041000
89. Grunwald V, Ngo HD, Formanski JP, et al (2023) Development of Zika Virus E Variants for Pseudotyping Retroviral Vectors Targeting Glioblastoma Cells. International Journal of Molecular Sciences 24:14487. https://doi.org/10.3390/ijms241914487
90. Liu J, Mao Y, Li Q, et al (2022) Efficient Gene Transfer to Kidney Using a Lentiviral Vector Pseudotyped with Zika Virus Envelope Glycoprotein. Hum Gene Ther 33:1269–1278. https://doi.org/10.1089/hum.2022.053
91. Ku MW, Anna F, Souque P, et al (2020) A Single Dose of NILV-Based Vaccine Provides Rapid and Durable Protection against Zika Virus. Mol Ther 28:1772–1782. https://doi.org/10.1016/j.ymthe.2020.05.016
92. Boigard H, Alimova A, Martin GR, et al (2017) Zika virus-like particle (VLP) based vaccine. PLOS Neglected Tropical Diseases 11:e0005608. https://doi.org/10.1371/journal.pntd.0005608